Copy
RM L53E26a

NACA

RESEARCH MEMORANDUM

PRELIMINARY RESULTS OF SUPERSONIC-JET TESTS OF SIMPLIFIED WING STRUCTURES

By Richard R. Heldenfels and Richard Rosecrans

Langley Aeronautical Laboratory
Langley Field, Va.

NATIONAL ADVISORY COMMITTEE FOR AERONAUTICS

WASHINGTON

July 8, 1953

NACA RM L53E26a

NATIONAL ADVISORY COMMITTEE FOR AERONAUTICS

RESEARCH MEMORANDUM

PRELIMINARY RESULTS OF SUPERSONIC-JET TESTS OF SIMPLIFIED WING STRUCTURES

By Richard R. Heldenfels and Richard Rosecrans

SUMMARY

Seven small multiweb wing structures were tested under simulated supersonic flight conditions to investigate the structural effects of aerodynamic heating. Three models experienced chordwise flutter and failure; the other four incorporated structural modifications that prevented flutter. The tests are discussed and the conclusion is reached that the models failed as a result of the combined action of aerodynamic heating and loading.

INTRODUCTION

As part of an investigation of the effects of aerodynamic heating on aircraft structures, the Langley Structures Research Division is testing multiweb wing structures under aerodynamic conditions similar to those encountered in supersonic flight. The first such test was made to obtain data on the temperature distribution in a small multiweb wing structure; however, the aerodynamic loads played an important and unanticipated role in that the model experienced a dynamic failure near the end of the test. Additional tests have been made to gather information on the nature and causes of failure and to investigate some design changes that might prevent failure. In this paper the tests conducted to date are described and the results are presented with the aid of diagrams, photographs, and observations based on motion-picture studies. The probable causes of the failures obtained are also indicated.

TEST CONDITIONS

An NACA facility at the Pilotless Aircraft Research Station on Wallops Island, Va. was used for these tests. This facility is a blowdown jet that incorporates a heat accumulator for stagnation-temperature

control. The models are placed in the free jet at the exit of a Mach number 2, 27- by 27-inch nozzle. During a typical test, the stream static pressure is maintained at about one atmosphere and the free-stream temperature at about 75° F. The corresponding stagnation temperature of 500° F provides a temperature potential of 425° that is available to heat the model. These conditions can be maintained in the jet for about 9 seconds following a 2-second starting period. An additional 3 seconds are required to shut down the jet, so that the total elapsed time is 14 seconds per test.

If the model is assumed to be a full-scale structure, the test then accurately reproduces both the aerodynamic heating and loading that would be experienced during a short flight at Mach number 2 at sea level on a warm day, a rather severe condition. If, however, the model is assumed to be only a quarter-scale structure, the test then reproduces the heating experienced by a full-scale airplane flying at Mach number 2 at 40,000 feet for about $2\frac{1}{2}$ minutes. The local air pressures, however, do not follow the same similarity laws as the heating and would be exaggerated by a factor of four on the quarter-scale model. (Some nondimensional parameters that establish similarity conditions for this type of testing are discussed in the appendix.)

RESULTS

Model MW-1

The test of model MW-1 is discussed in reference 1; however, the test is reviewed herein so that the rather startling results can be interpreted in view of more recent tests.

The model chosen for the first test was a somewhat idealized section of an untapered multiweb wing as shown in figure 1. The airfoil section was a 5-percent-thick symmetrical circular arc and the model was constructed of 24S-T3 aluminum alloy except for the bulkheads and mounting fixtures which were of steel. The model was mounted vertically in the jet at an angle of attack of 0° with its leading edge just downstream of the nozzle exit plane. The model extended completely through the jet with about 2/3 of the span in the airstream.

After the jet started, the model remained stationary for approximately $7\frac{1}{2}$ seconds; then, a vibratory motion started and the model was soon destroyed. About $1\frac{1}{2}$ seconds elapsed between the first sign of distress and the first failure, an additional second being required for the progressive destruction of the model.

Motion pictures of the test showed that the first sign of distress was skin buckling near the leading edge. The buckles appeared and disappeared rapidly, moving toward the trailing edge. A buckle then settled in the most rearward skin panel. This panel tore out along rivet lines, the trailing edge piece blew away and progressive disintegration followed until destruction was completed.

A study of this failure indicates that the rapid heating of the model must have been the primary cause of failure or the model would have shown some sign of distress earlier in the test. When the test started, the model was at 50° F, but eight seconds later the skin near the leading edge had reached 332° while parts of the internal structure had risen to only 80°. The temperature distribution in this model is discussed in more detail in references 1 and 2. For the present purpose, it is sufficient to know that the model temperatures increased at a rapid rate and varied greatly throughout the model.

The principal structural effect of this rapid, nonuniform heating was that substantial thermal stresses were induced in the model, including compressive stresses in the chordwise direction sufficient to buckle the skin. These particular stresses result from the restraint provided by the bulkheads located outside the jet. The buckled model skin apparently created an unstable aeroelastic condition that resulted in some form of localized flutter. Initially, it was thought that panel flutter may have caused the failure, but the available data on panel flutter and subsequent tests of similar models indicate that the phenomenon observed in this test was not the form of panel flutter discussed in reference 3, but a more complex type of flutter.

Model MW-2

The test of Model MW-1 yielded very little data on the failure and in itself was not conclusive because of certain peculiarities of the model and its supports. Additional tests were conducted with smaller models like that shown in figures 2 and 3. These models represented small wings of 20-inch chord and span and extended into the jet from a support somewhat representative of the side of a fuselage, passing through a plate parallel to and just inside the lower jet boundary. The models lacked seven inches of spanning the jet. All models had 5-percent-thick, symmetrical circular-arc airfoil sections.

The table presented as figure 4 lists some significant dimensions of the various models tested. The model numbers are listed in the first column. The other columns give the material, the skin thickness t_S, the thickness of the internal spanwise webs t_W, the thickness of internal chordwise ribs t_R, if any, and finally the thickness of the tip bulkhead t_B, all dimensions being in inches. Thus, the second model was

[redacted]

constructed of 24S-T3 aluminum alloy and it had a skin thickness of 0.064 inch. The internal webs were 0.025 inch thick, and no internal ribs were used, but a 0.25-inch bulkhead was placed at the tip.

The second model (MW-2) was essentially a half-size version of the first model, although some of the construction details were changed. This model was tested in the same manner as model MW-1, and although its thinner skin heated faster, it survived longer. The first evidence of distress was buckling of the most rearward skin panel about 10 seconds after the test started. The tip of the trailing edge separated about $1\frac{1}{2}$ seconds later and successive pieces were peeling off when the air supply was exhausted 14 seconds after the test started. If the jet had continued to run, the model probably would have been completely destroyed.

In the motion pictures of the test, the skin buckle, near the tip and just forward of the trailing-edge member, seemed stationary, but close study revealed a definite suggestion of vibration. The same sequence of events was observed in both side views of the model, that is, skin buckling, vibration, and successive disintegration. The top view, however, showed that the model was fluttering prior to failure and that the initial fracture included a part of the tip bulkhead. The flutter continued as the model broke up. The vibrations were particularly severe while the jet was shutting down, but this latter action is a characteristic of the jet and is not associated with the heating or failure of the model.

Figure 5 shows model MW-2 as it appeared after the test. The extent of the failure and the manner in which the model was mounted in front of the nozzle exit can be seen. The two masts downstream of the model were used to support stagnation temperature probes which were broken off by fragments of the model.

The failure of this second model was fundamentally the same as that of the first in that skin buckling induced the model to flutter and then fail. Certain differences were evidenced in the shape of the buckle and the longer time required to induce failure. These differences can be explained in part by the change in detail design, particularly in the tip region, and the resulting changes in the thermal stress distribution.

The skin of this model was heated very rapidly, a point near the leading edge rising from 74° F to 400° F in 10 seconds, at which time the skin temperature was beginning to stabilize although some of the webs had risen to only 240° F. This temperature distribution induced thermal stresses in the model, particularly compressive stresses in the hot skin. Differential expansion between the skin and webs caused compression in the spanwise direction, whereas the restraint offered by the tip and root ribs created compression in the chordwise direction. Approximate calculations and the recorded strains indicated that these two types

of stresses were of about the same order of magnitude, around 6000 psi. The chordwise stresses were the more important, however, because the stresses in this direction were of the same order of magnitude as the critical chordwise compressive stress. This critical stress was only 1/4 of the critical stress in the spanwise direction because of the long narrow skin panels. The concentration of the buckling near the tip indicates that the tip rib was a major factor, an observation further supported by the fact that the initial fracture was apparently a tension failure of the tip rib at a section weakened by several rivet holes.

The strain-gage data collected during this test provided some approximate values of the static thermal stresses, as mentioned before, but these data are not very reliable because of large temperature effects on the strain gages. These data shed additional light on the failure, however, in that they give the frequency and phasing of vibrations of some parts of the model. At the time of failure, the model was fluttering at about 230 cycles per second. The model did not experience flutter of the individual panels, but a chordwise mode in which the airfoil section vibrated with about $1\frac{1}{2}$ waves along the chord and with the maximum amplitude in the vicinity of the trailing edge. Thus, the motion pictures of the test show this flutter as a "tail-wagging" action.

The results of this test indicate that the immediate cause of failure, chordwise flutter, was induced by thermal buckling of the model skin. If this analysis is correct, then, both flutter and the resulting failure should not occur if buckling is prevented. Structural changes that may prevent buckling are an increase in skin thickness, a reduction in the stiffness of the tip rib, or the addition of transverse ribs. Each of these changes has been incorporated in a test model. Changes in the root connection have not yet been investigated because the test of model MW-2 indicated that the buckling occurred in the tip region.

Model MW-3

Model MW-3 was nearly identical to model MW-2, as shown in figures 2 and 4, except for the skin thickness which was increased from 0.064 to 0.081 inch. This change not only increased the critical stress of the skin but also decreased the thermal stresses induced during the test. This model showed no signs of distress when tested at zero angle of attack. The 27-percent increase in skin thickness was thus sufficient to prevent buckling and failure. This model was also tested at angles of attack of 1.5° and 3° and survived both without difficulty. In the final test at an angle of attack of 5°, however, the model failed statically. This failure was expected since the calculated aerodynamic loads were about 1000 pounds per square foot, enough to cause compressive buckling of the skin near the root.

[redacted]

The motion pictures of the final test of model MW-3 showed that the model vibrated during the starting period, stabilized as soon as supersonic flow was established, and then fell over when the dynamic pressure reached the prescribed test value. (The vibrations, experienced by this and other models whenever the jet starts or stops, occur while a normal shock is inside the nozzle. They have a random variation of amplitude and are principally bending oscillations, although a few small torsional oscillations also occur.)

Model MW-4

Model MW-4 was similar to model MW-2 except for a change in the tip bulkhead, a light bulkhead 0.025 inch thick being used instead of the 0.25-inch bulkhead on model MW-2. This change was expected to reduce the thermal stresses in the tip region and prevent skin buckling. This model showed no particular evidence of buckling during the test, but it went into a chordwise flutter mode about 5 seconds after the jet started.

The movies of this test showed the usual initial model vibrations associated with jet starting. The model then remained stationary until a hint of trouble occurred, after which it was suddenly torn off at the root. High-speed motion pictures taken at 650 frames per second, however, clearly show the chordwise flutter mode of about $1\frac{1}{2}$ waves along the chord. The flutter increased in severity until the airfoil section became greatly distorted. The model then began to bend and a fracture started at the leading edge near the root. This fracture quickly proceeded to the trailing edge, severing the model from the supporting structure. Less than 1/2 second elapsed between the inception of flutter and the failure of the model.

The chordwise flutter mode of about $1\frac{1}{2}$ waves along the chord can be seen in figure 6 which presents two consecutive frames from the 650-frames-per-second motion picture. The model, which was painted with a grid to aid observation, is viewed from above and to one side; the air flowed from left to right. At the time these pictures were made, the flutter had become severe and the model was completely separated from the supporting structure 12 frames later.

The analysis of this test has not yet been completed, but the preliminary results show that model MW-4 was fluttering at 240 cycles per second, about the same frequency as model MW-2. The amplitudes were larger on model MW-4, however, because the light tip bulkhead offered very little resistance to chordwise distortion. The large reduction in the stiffness of the tip bulkhead was thus completely ineffective in preventing failure since the failure occurred sooner and more violently.

[redacted]

Nevertheless, the lack of skin buckling indicates that the use of a light tip bulkhead did reduce the chordwise thermal stresses induced in the model.

In the case of models MW-1 and MW-2 it was concluded that flutter was incited by skin buckling, but in the case of model MW-4 flutter was obtained without obvious buckling of the model skin. A change in the effective stiffnesses (and thus in natural frequencies) of a model may incite flutter. Skin buckling of models MW-1 and MW-2 made an obvious change in the effective stiffness; whereas in model MW-4 a more subtle stiffness change must have taken place because of the spanwise thermal stresses induced in the model; especially the compressive stresses in the skin. Model MW-4 was particularly susceptible to a critical stiffness change because of its low initial chordwise stiffness.

Models MW-5 and MW-6

Models MW-5 and MW-6 incorporated chordwise ribs as shown in figures 3 and 4. These ribs were the same distance apart as the webs, forming square skin panels, so that the critical stress in the chordwise direction was raised to a safe value. Model MW-5 was similar to model MW-2 except for the ribs, whereas model MW-6 had a thinner skin, with a thickness of 0.050 inch instead of 0.064 inch. The thinner skin should lead to higher thermal stresses and lower critical values; however, the stresses should still not exceed the critical. Each model was tested at an angle of attack of 0° and survived the test in good condition.

In addition to preventing thermal buckling of the skin, the use of internal ribs further discourages chordwise flutter because of the extra stiffness provided. Some of the natural modes of vibration of models MW-4 to MW-7 were determined experimentally and those without internal ribs experienced modes involving cross-sectional distortion at much lower frequencies than those with ribs. All models had first bending and torsional natural frequencies at about 60 and 145 cycles per second, respectively. The second bending frequency of the ribbed models (295 cps) was easily determined, but it was not found for the ribless ones because of the more predominant modes (at 265 and 380 cps) involving cross-sectional distortion.

Model MW-7

The last model (model MW-7) to be discussed was similar to model MW-2 but the material was changed, mild steel being used instead of aluminum alloy. The change in material was accompanied by a reduction in skin and web thicknesses such that the critical compressive stress of model MW-7 was about the same as that of model MW-2. The thicknesses of steel used

were 0.043 inch for the skin and 0.018 inch for the webs. Thus, model MW-7 weighed over twice as much as model MW-2 but had only slightly more static strength. The changes should have resulted in high thermal stresses in model MW-7, so that the skin was expected to buckle and initiate chordwise flutter of the model. Model MW-7 did not react as expected, however, and survived the test in good condition. Nevertheless, there was some slight evidence of surface distortion at the end of the test. Analysis of this test is as yet incomplete and the preliminary results have failed to reveal the conditions that prevented thermal buckling; however, the change of material was, without doubt, an important factor.

CONCLUDING REMARKS

In conclusion, seven small multiweb wing structures have been tested under simulated supersonic flight conditions. Models MW-1, MW-2, and MW-4 failed dynamically as a result of chordwise flutter. This flutter was incited apparently by a reduction in the effective stiffnesses (and thus natural frequencies) of the model due to thermal stresses and distortions that were, in turn, induced by aerodynamic heating. These three models were basically alike but incorporated different tip bulkheads. The characteristics of the failure were affected by the changes in chordwise stiffness, with model MW-4 (the one with the lightest tip bulkhead) experiencing the most violent flutter. The other models were similar to model MW-2 but incorporated structural modifications that prevented flutter. Thus the thicker skin of model MW-3, the internal ribs of model MW-5, and the steel material used in model MW-7 were each effective. The internal ribs were not only effective in preventing flutter of model MW-5, which had the same skin thickness as model MW-2, but they also prevented flutter of model MW-6 which had even thinner skin. From the weight standpoint, the use of internal ribs was the most efficient method of preventing flutter of the particular configuration investigated. On the other hand, the conversion to steel resulted in a twofold increase in the weight of that part of the structure exposed to the jet. The use of internal ribs, however, may not be the most efficient method of preventing chordwise flutter of other multiweb wing designs. It is also well to point out that all these tests were of very brief duration and that the models were still experiencing transient heating when the air supply was exhausted; thus, they may not have survived a longer test.

Research on the structural problems associated with transient aerodynamic heating is still in its early stages, but the implications of the tests described here are clear. The effects of aerodynamic heating

and loading on aircraft structures must be considered as a single, combined problem, or factors which vitally affect the structural integrity of an aircraft may be overlooked.

Langley Aeronautical Laboratory,
National Advisory Committee for Aeronautics,
Langley Field, Va., May 15, 1953.

[redacted]

APPENDIX

SOME SIMILARITY PARAMETERS APPLICABLE TO SUPERSONIC JET TESTS OF STRUCTURAL MODELS

The results of the tests described in this paper may be applied directly to the design of aircraft and missile structures if certain similarity conditions are satisfied. Some of the nondimensional parameters that establish similarity of strains, temperatures, aerodynamic heating, and aerodynamic loading have been derived by dimensional analysis with the results given in this appendix. The equations show the requirements for true similarity but fail to indicate the relative importance of the various parameters or how test results are effected by deviations from similarity.

Only a few pertinent quantities have been included in this analysis, many others could be used but have been omitted for brevity. The analysis has been further simplified by assuming that the model is tested in air and is geometrically similar to and made of the same material as the full-scale structure, conditions usually required for structural tests. A list of symbols is given at the end of this appendix.

Equations

Functional relationships between the nondimensional parameters that apply to each of the phenomena being considered are expressed by the following equations:

Strain distribution in the structure:

$$\epsilon = f\left(\alpha_s T_I,\ \frac{p}{E},\ \frac{wl}{E}\right) \tag{A1}$$

Temperature distribution in the structure:

$$\frac{T_I}{T_{AW}} = f\left(\frac{T_o}{T_{AW}},\ \frac{k_s t}{c w l^2},\ \frac{hl}{k_s}\right) \tag{A2}$$

[redacted]

Aerodynamic heating of the structure:

$$\frac{hl}{k_a} = f\left(\frac{T_s}{T_w}, \frac{\rho V l}{\mu}, \frac{V}{a}\right) \tag{A3}$$

Aerodynamic loads on the structure:

$$\frac{p}{\rho V^2} = f\left(\alpha, \frac{\rho V l}{\mu}, \frac{V}{a}\right) \tag{A4}$$

Discussion

Examination of the equations (A1) to (A4) shows that for these tests, as for any type of model test involving different physical phenomena, many requirements are contradictory so that complete similarity can be attained only under full-scale conditions. In this paper, the structural effects of aerodynamic heating are of primary interest; therefore, the equations will be examined with respect to similarity of structural strains due to changes in the temperature distribution.

Equation (A1) indicates that the temperature distribution in the structure should be the same in the model as in the full-scale structure if the strains are to be similar. To achieve the required temperature distribution, then, the temperature of the airstream and the Fourier and Biot numbers for the structure should be the same (equation (A2)). The Fourier number relates the time scale of the model to full-scale conditions, thus

$$t_M = n^2 t_F \tag{A5}$$

where n is a scale factor so defined that

$$l_M = n l_F \tag{A6}$$

The Biot number of the structure will be the same if the Nusselt number of the airstream is the same for both model and full-scale conditions. This requirement is met if the temperature of the air and the Reynolds and Mach numbers, given in equation (A3), are maintained, that is,

[redacted]

$$V_M = V_F \tag{A7}$$

$$\rho_M = \frac{1}{n} \rho_F \tag{A8}$$

The requirement on density, equation (A8), can be converted to pressure by using the equation of state, with the following results

$$p_M = \frac{1}{n} p_F \tag{A9}$$

The above relations (equations (A5) to (A9)) establish similarity of temperature distribution and the associated strains. The maintenance of Reynolds and Mach numbers also provides similarity, on a nondimensional basis, of the aerodynamic loads, equation (A4). The structural strains produced by these loads will not, however, be similar in model and full-scale structures because equation (A1) requires that

$$p_M = p_F \tag{A10}$$

which is contrary to equation (A9) except at full-scale. Therefore, if temperature similarity is maintained, the local aerodynamic loads on the scale model will not be of the same relative magnitude as those in the full-scale structure.

Equation (A1) also shows that the strains due to a distributed inertia load are not properly simulated on a geometrically scaled model of the same material as the full-scale structure. The results of the tests described in this paper can therefore be applied to other structures under only limited conditions. The temperature distributions measured in the model can be interpreted in terms of larger aircraft flying at higher altitudes if the time scale is properly adjusted. The effects of the aerodynamic loads and the dynamic characteristics of the model do not, however, follow the same similarity laws so that the complete results of the tests cannot be extrapolated in a simple manner.

Symbols

a	speed of sound in air, ft/sec
c	specific heat of structural material, Btu/(lb)($^{\circ}$R)
E	modulus of elasticity of structural material, psi
h	boundary-layer heat-transfer coefficient, Btu/(sq ft)(sec)($^{\circ}$R)
k_a	thermal conductivity of air, Btu/(ft)(sec)($^{\circ}$R)
k_s	thermal conductivity of structural material, Btu/(ft)(sec)($^{\circ}$R)
l	characteristic dimension of structure, ft or in.
l_M	characteristic dimension of model structure, ft or in.
l_F	characteristic dimension of full-scale structure, ft or in.
n	scale factor $\left(n = \frac{l_M}{l_F}\right)$
p	static pressure, lb/sq ft or lb/sq in.
t	time, sec
T_{AW}	adiabatic wall temperature, $^{\circ}$R
T_I	internal temperature of structure, $^{\circ}$R
T_o	initial temperature of structure, $^{\circ}$R
T_S	stagnation temperature, $^{\circ}$R
T_W	surface temperature of structure, $^{\circ}$R
V	airspeed, ft/sec
w	specific weight of structural material, lb/cu ft or lb/cu in.
α	angle of attack, degrees or radians
α_s	coefficient of linear thermal expansion of structural material, in./(in.)($^{\circ}$R)

[redacted]

ϵ	strain in structure, in./in.
μ	viscosity of air, slugs/ft-sec
ρ	density of air, slugs/cu ft
$\frac{k_s t}{c w l^2}$	Fourier number
$\frac{h l}{k_s}$	Biot number
$\frac{h l}{k_a}$	Nusselt number
$\frac{\rho V l}{\mu}$	Reynolds number
$\frac{V}{a}$	Mach number

[redacted]

REFERENCES

1. Heldenfels, Richard R., Rosecrans, Richard, and Griffith, George E.: Test of an Aerodynamically Heated Multiweb Wing Structure (MW-1) in a Free-Jet at Mach Number Two. NACA RM L53E27, 1953.

2. Griffith, George E.: Transient Temperature Distribution in an Aerodynamically Heated Multiweb Wing. NACA RM L53E27a, 1953.

3. Sylvester, Maurice A., and Baker, John E.: Some Experimental Studies of Panel Flutter at Mach Number 1.3. NACA RM L52I16, 1952.

[redacted]

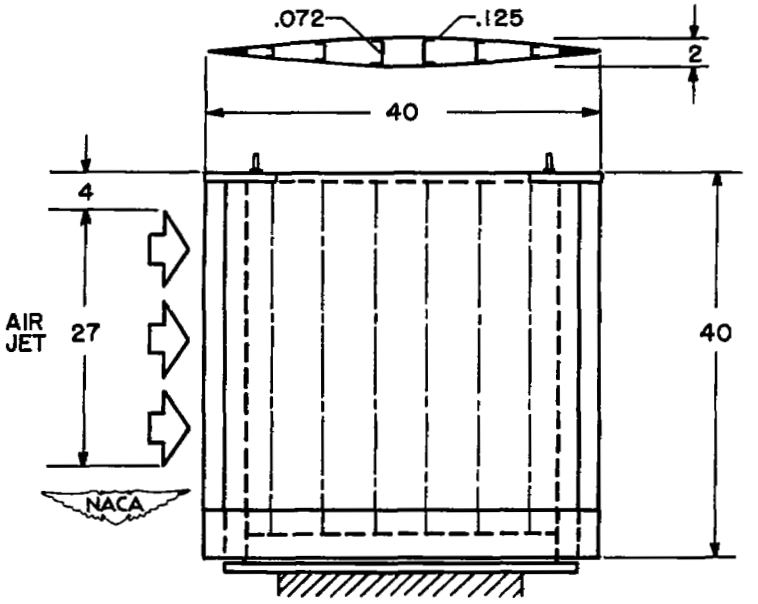

Figure 1.- Configuration of model MW-1.

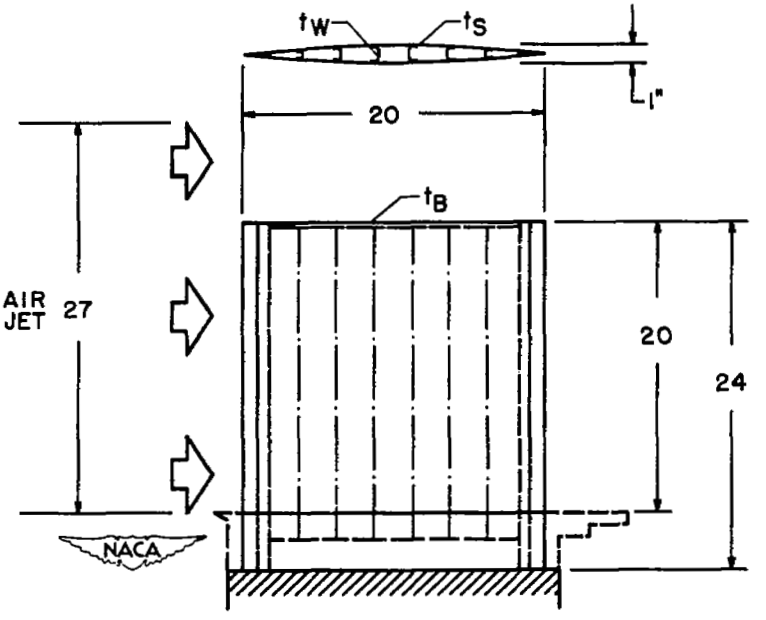

Figure 2.- Configuration of models MW-2, -3, -4, and -7.

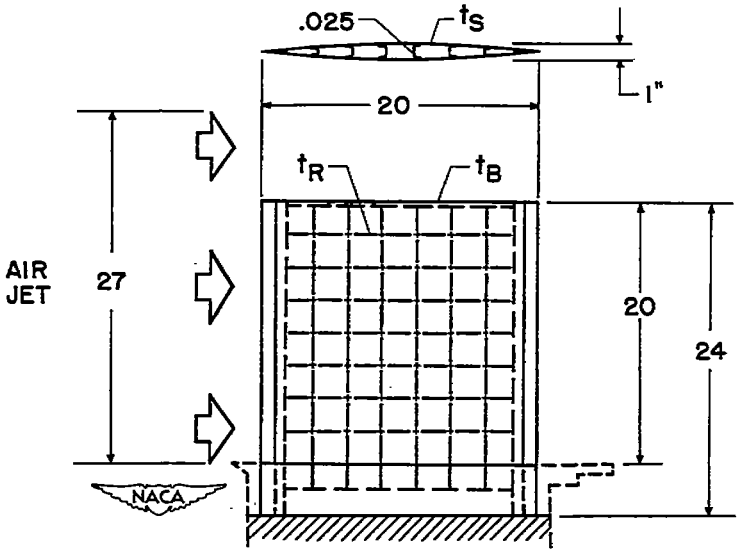

Figure 3.- Configuration of models MW-5 and -6.

MODEL	MAT.	t_S	t_W	t_R	t_B
1	24S-T3	0.125	0.072	—	1*
2		.064	.025	—	.25
3		.081		—	.25
4		.064		—	.025
5		.064		0.025	.25
6		.050		.025	.25
7	STEEL	.043	.018	—	.25

NACA

* STEEL BULKHEAD

Figure 4.- Summary of model dimensions.

[redacted]

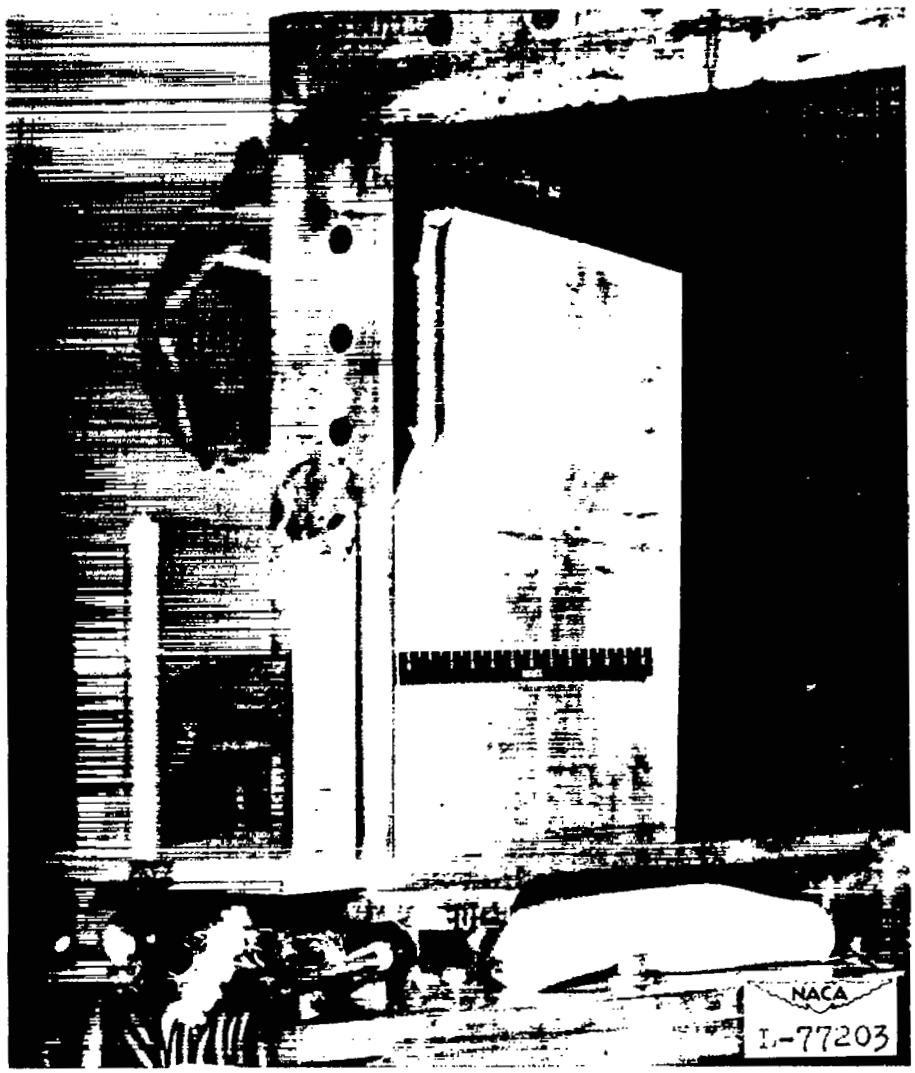

Figure 5.- Remains of model MW-2, in place at nozzle exit, after test.

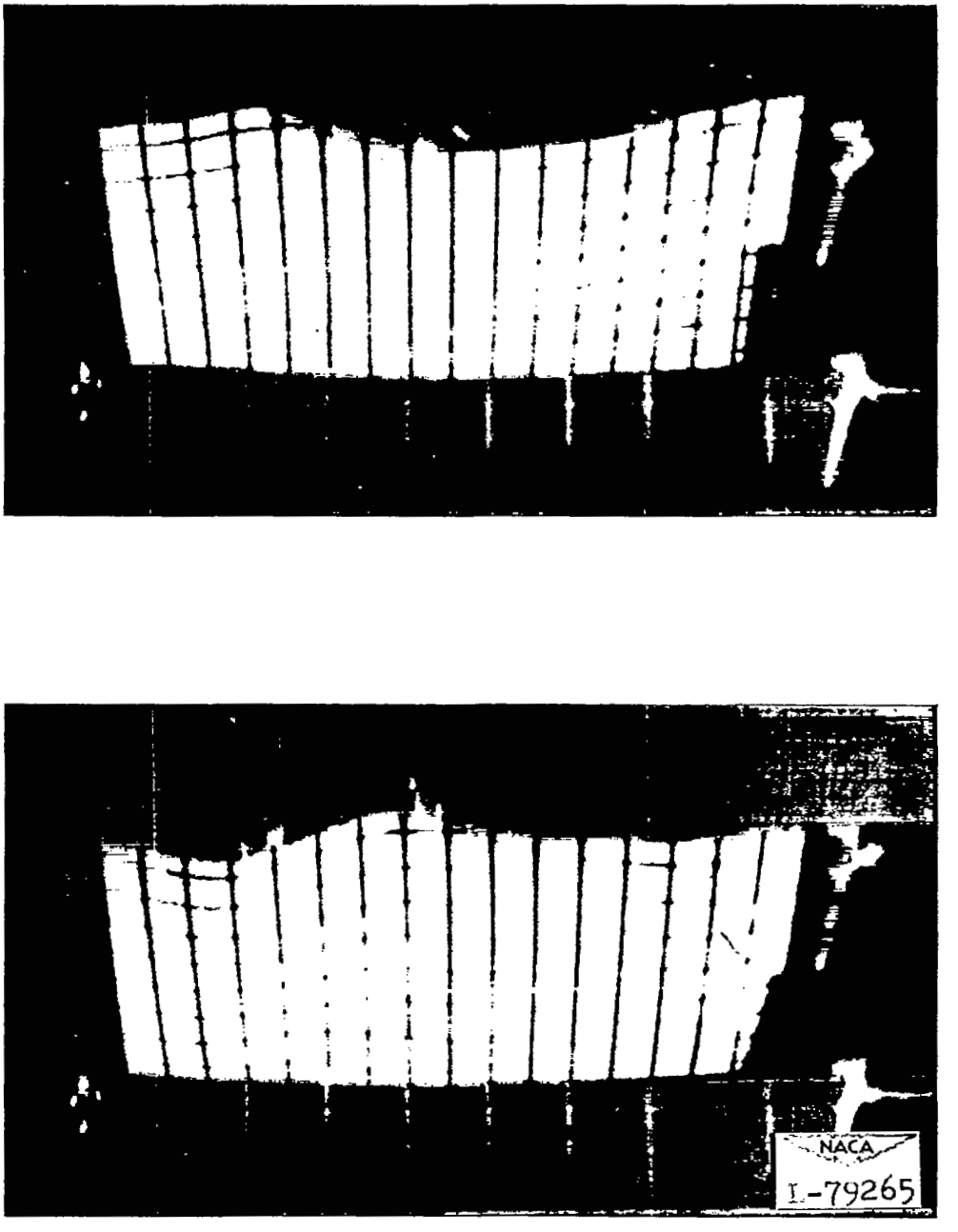

Figure 6.- Distortion of model MW-4 just prior to failure (taken from consecutive frames of motion picture).

[redacted]

[redacted]